

Optical bistability and cooperative effects in resonance fluorescence

R. Bonifacio* and L. A. Lugiato

Istituto di Fisica dell'Università, Via Celoria, 16, 20133 Milano, Italy

(Received 15 August 1977)

We discuss a mean-field quantum-mechanical model which describes the dynamics of a homogeneously broadened system of two-level atoms contained in a pencil-shaped resonant cavity and driven by a coherent resonant field E_I . The model is treated in the semiclassical approximation. The model is justified on the basis of Maxwell-Bloch equations with two coherently coupled directions of propagation, with boundary conditions for the fields taken into account. Above a suitable critical density of atoms the system exhibits a bistable behavior including both the stationary situation and the transient, both the light transmitted in the forward direction and the fluorescent light. Bistability is shown to be a consequence of atomic cooperation. We give a simple description of optical bistability leading to new predictions for the transient behavior of the transmitted light and for the spectrum of the fluorescent light. The damping constant which characterizes the rate of approach to the stationary situation exhibits a hysteresis cycle. In the low-transmission regime the approach is monotonic, whereas in the highly transmitting situation the approach is oscillatory. One finds a critical slowing down in correspondence with the values $E_I^{(+)}$, $E_I^{(-)}$ of the incident field where the transmitted field (as well as the total fluorescence intensity, the rate of approach to the stationary state, etc.) changes discontinuously. On the basis of the regression hypothesis we give a qualitative description of the spectrum of the fluorescent light. This is shown to undergo hysteresis and discontinuous changes at the same values $E_I^{(+)}$, $E_I^{(-)}$ of the incident field. Below the critical density of atoms one recovers the usual picture of resonance fluorescence, with a continuous transition from a single-line spectrum to a three-peaked structure when the Rabi frequency becomes equal to the *natural* linewidth. Above the critical density the triplet appears only when the Rabi frequency becomes equal to the *cooperative* linewidth of pure super-fluorescence (i.e., for $E_I = E_I^{(+)}$). Moreover, it appears discontinuously: when E_I crosses the value $E_I^{(+)}$ the spectrum changes from a single narrow line to a triplet with well-separated sidebands.

I. INTRODUCTION

Cooperative phenomena in open systems far from equilibrium are presently the object of an ever increasing interest.¹ At a phenomenological level, they are described by a set of nonlinear equations with suitable damping terms. The interplay of nonlinearity and dissipation alone gives rise to a large variety of phenomena. Among them, one of the most interesting possibilities is the appearance of phase transitions in open systems lying in stationary nonequilibrium states. As usual, exactly soluble models are essential to obtain insight into the physics of these phenomena, as well as to discover connections between different phenomena. A typical example is the one-mode laser model with distributed losses,² which exhibits a second-order phase transition.³ In this paper we illustrate a soluble quantum mechanical model which shows a *first*-order phase transition.⁴ It is a simple generalization of the one-mode laser model which includes the effect of an external coherent field that continuously drives the atoms. We put ourselves in the simplest situation, i.e., we assume that the frequency of the injected field is perfectly tuned with the optical cavity and consider a homogeneously broadened atomic system perfectly in resonance with the driving field.

In the present paper we treat our model in the

semiclassical approximation. The semiclassical formulation can be clearly deduced from the Maxwell-Bloch equations, taking into account the boundary conditions for the propagating field and performing the mean-field approximation. The model gives a unified description of different phenomena such as optical bistability, resonance fluorescence, and superfluorescence and allows a clear analysis of the role of atomic cooperation in all of them. More precisely, the results that one finds using the present model are the following:

(i) We give a simple description of optical bistability.⁵ This phenomenon, which recently has been experimentally observed,⁶ consists of the fact that under suitable conditions the light amplitude E_T transmitted by a filled optical cavity can vary discontinuously with the incident field amplitude E_I , showing a hysteresis cycle (see Fig. 1). In fact, for low incident field the transmission is very low, so that almost all the incident light is reflected. Increasing the incident field one finds that in correspondence with a suitable value $E_I = E_I^{(+)}$ the transmitted light increases discontinuously. If, conversely, one decreases E_I starting from values $E_I > E_I^{(+)}$, one sees that the transmitted light decreases continuously until in correspondence with a second transition value $E_I^{(-)} < E_I^{(+)}$ the transmitted field suddenly jumps downwards, closing the cycle. This behavior is due to the fact

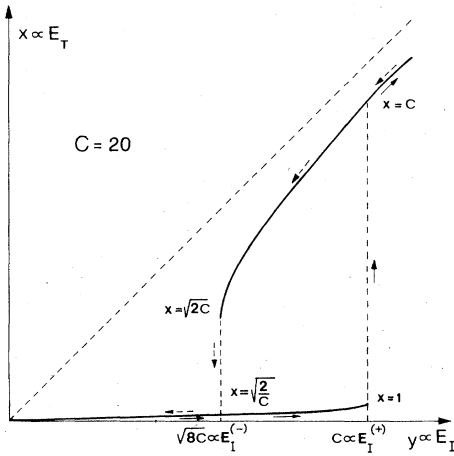


FIG. 1. Hysteresis cycle of the transmitted light. Full (dotted) line arrows indicate the variations obtained increasing (decreasing) the injected field E_I . The upper part of the plot corresponds to the one-atom stationary solution, the lower part corresponds to the cooperative stationary solution.

that the two branches in Fig. 1 correspond to two different stable stationary states of the system (bistability). As is well known, hysteresis is one of the main characteristic features of first-order phase transitions. Whereas the theory of Ref. 5 gives only numerical results, the present treatment is completely analytical. In particular, it gives an explicit condition for the appearance of the bistable behavior and explicit expressions for the values of the input field at which the discontinuities occur.

One finds a direct connection between atomic cooperation and bistable behavior. In fact, the condition for the appearance of the bistable behavior is

$$\gamma_R > 8\gamma_L, \quad (1.1)$$

where $\gamma_L = T_2^{-1}$ is the incoherent transverse atomic relaxation rate, while γ_R is the cooperative damping rate of pure superfluorescence.⁷ Since γ_R is proportional to the atomic density, the bistable behavior appears when the density is high enough so that atomic cooperation can overcome the incoherent single-atom processes. Actually Eq. (1.1) fixes a critical value of the density below which no bistable behavior can arise. So bistability is just the stationary counterpart of transient cooperative spontaneous emission, or superfluorescence, for a system coherently and continuously excited. More specifically, the analysis shows that in the bistable situation one of the two stable steady states corresponding to a given value E_I arises from atomic cooperation (low transmission branch of Fig. 1); for this reason it will be called "cooperative stationary state." The

other stable steady state does not exhibit cooperative behavior (high transmission branch of Fig. 1); we will refer to it as the "one-atom stationary state." The discontinuity points $E_I^{(+)}$, $E_I^{(-)}$ correspond roughly⁸ to the situations $\Omega_I = \gamma_R$ and $\Omega_I = (\gamma_R \gamma)^{1/2}$, where Ω_I is the Rabi frequency of the injected field and γ is the natural linewidth of the atoms. When the system is in the one-atom stationary state and $E_I \gtrsim E_I^{(+)}$, the transmitted intensity is independent of N and practically coincides with the incident intensity. In contrast, when the system is in the cooperative stationary state the transmitted field amplitude is inversely proportional to the number of atoms.

We give completely new predictions concerning the transient behavior of the system, and in particular of the transmitted light. A rigorous and complete stability analysis shows that there is a critical slowing down in correspondence with the discontinuity points $E_I^{(+)}$, $E_I^{(-)}$ of the hysteresis cycle. The approach to the cooperative stationary state is monotonic and becomes slower and slower as E_I approaches $E_I^{(+)}$. Increasing E_I slightly beyond $E_I^{(+)}$, one has an abrupt increase in the relaxation rate to the steady state, which now is the one-atom stationary state. When the cavity damping constant is larger than the atomic relaxation rates, the approach to the one-atom stationary state is oscillatory: the damping rate is the mean value of the atomic relaxation rates $\gamma_1 = T_1^{-1}$, $\gamma_2 = T_2^{-1}$ and the frequency coincides with the Rabi frequency Ω_I . If, conversely, the incident field is decreased, starting from a value larger than $E_I^{(+)}$, the oscillatory approach to the one-atom stationary state becomes gradually monotonic when E_I gets close to $E_I^{(-)}$ and simultaneously the relaxation rate becomes smaller and smaller because of the critical slowing down. Finally crossing the transition value $E_I^{(-)}$ from above, there is again an abrupt increase in the relaxation rate. Hence, one also finds a hysteresis cycle in the transient behavior of the system.

(ii) The model describes the impact of atomic cooperation on resonance fluorescence, showing that the usual one-atom theory of resonance fluorescence⁹ is valid only below the above-mentioned critical density of atoms. In contrast, above the critical density the system exhibits a bistable behavior which concerns not only the transmitted light but also the fluorescent light. In fact, both the *total fluorescent light and the spectrum* of the fluorescent light show a hysteresis cycle.

(a) When the system is in the one-atom stationary state, the total fluorescence intensity is proportional to the number of atoms, which is the normal situation. On the contrary, when the system is in the cooperative stationary state the total

fluorescence intensity turns out to be inversely proportional to the number of atoms. This striking cooperative effect is just the opposite of what occurs in superfluorescence, in which atomic cooperation gives rise to a radiation output proportional to the square of the number of atoms.

(b) According to the one-atom theory of resonance fluorescence⁹ the spectrum becomes three-peaked (dynamical Stark shift, DSS) in a continuous way as the intensity of the external field is increased. In fact the two sidebands gradually emerge from the central line when $\Omega_I \sim \gamma$. This is a kind of second-order phase transition. In our theory, using the regression hypothesis we tentatively associate the linewidth and the shift to the real and imaginary parts of the damping constants given by the linear stability analysis. In such a way we obtain a qualitative description of the spectrum. This shows that when the bistability condition (1.1) is satisfied one should find a spectral hysteresis cycle. Namely, when the cavity damping constant k is much larger than γ , the resulting picture is the following: The spectrum remains single peaked whenever the system is in the cooperative stationary state. Hence, no DSS appears when Ω_I becomes larger than γ , provided Ω_I remains smaller than γ_R . Also, one finds a line narrowing as Ω_I approaches γ_R from below (i.e., approaching the discontinuity point $E_I^{(+)}$). This cooperative line narrowing is connected to the critical slowing down mentioned above. Only when crossing the value $\Omega_I = \gamma_R$ (i.e., jumping to the one-atom stationary state) one finds an abrupt appearance of the three-peaked spectrum, with two already widely separated sidebands. The substitution of the condition $\Omega_I > \gamma$ by the condition $\Omega_I > \gamma_R$ for the appearance of the DSS is not surprising; what is striking is that the DSS arises discontinuously.

Conversely, if one starts from values of Ω_I larger than γ_R , the system lies in the one-atom stationary state and exhibits a large DSS. Decreasing Ω_I one finds that the spectrum becomes a single narrow line as the discontinuity point $E_I^{(-)}$ is approached from above. Hence when Ω_I approaches $(\gamma_R \gamma)^{1/2}$ from above there is a *continuous* disappearance of the DSS. This is again a remarkable cooperative effect since when $\gamma_R > \gamma$, then also $(\gamma_R \gamma)^{1/2} > \gamma$. Finally, when crossing the value $(\gamma_R \gamma)^{1/2}$ (i.e., jumping to the cooperative stationary state) one finds an abrupt line broadening but without any appearance of DSS.

In conclusion, these results suggest a certain number of experiments concerning both the transient behavior of the transmitted light and the stationary behavior of the fluorescent light. The semiclassical version of the model is presented

and illustrated in Ref. 2, while the deduction from the Maxwell-Bloch equations is shown in Appendix A. The fully quantum-mechanical model is given in Appendix B. In Sec. III we deduce the stationary solutions and show that when condition (1.1) is satisfied all the relevant macroscopic quantities exhibit a hysteresis cycle. The linear stability analysis of the stationary solutions, with the proof of the existence of a critical slowing down at the discontinuity points $E_I^{(+)}$, $E_I^{(-)}$, is given in Sec. IV. In Sec. V we treat the transient behavior of the system. The spectrum of the fluorescent light is finally discussed in Sec. VI. A preliminary version of the present work is given in Ref. 4.

II. MODEL

A coherent monochromatic field E_I of frequency ω_0 is injected into a pencil-shaped optical cavity of length L and volume V , such that L is equal to an integral number of wavelengths (i. e., zero cavity mistuning). The cavity has mirrors of reflectivity coefficient R , and contains $N \gg 1$ two-level atoms with transition frequency ω_0 (i.e., homogeneously broadened medium, no detuning with the incident field). Apart from the external field E_I no other mechanism to pump the atoms is considered in the present model. The atoms are assumed to be initially in the ground state. The coherent interaction between the field propagating along the longitudinal axis and the atoms is described as follows. Once entered into the cavity, the injected field induces a macroscopic polarization S and changes the population difference

$$\Delta = (N_1 - N_2)/2, \quad (2.1)$$

where N_1 (N_2) is the total population of the lower (upper) level. The polarization radiates in turn a reaction field which adds itself to the incident field giving rise to the total internal field E . Obviously the central frequency of S and E coincides with the frequency of the incident field. The incoherent atomic decay is characterized by the transverse and longitudinal relaxation rates $\gamma_1 = T_2^{-1}$, $\gamma_{||} = T_1^{-1}$. Our model equations are derived in Appendix A from the equations (Maxwell-Bloch type) which describe the interaction of matter with two fields propagating in opposite directions in the medium with coherent coupling between the two traveling waves. The derivation is based on the proper boundary conditions for the field⁵ and on suitable approximations which are quite reasonable when the transmittivity coefficient $T = 1 - R$ is small. The model consists of three coupled time-evolution equations for the real quantities S , Δ , and E , which are precisely and respectively defined as the space averages of the polarization, of the

population difference, and of the field propagating in the forward direction (i.e., the direction of the incident light). The equations are:

$$\dot{S} = (\mu/\hbar)E\Delta - \gamma_{\perp}S, \quad (2.2a)$$

$$\dot{\Delta} = -(\mu/\hbar)ES - \gamma_{\parallel}(\Delta - \frac{1}{2}N), \quad (2.2b)$$

$$\dot{E} = -gS - \kappa[E - (E_I/\sqrt{T})], \quad (2.2c)$$

where μ is the modulus of the atomic dipole moment times $\sqrt{3}$,

$$g = (4\pi\omega_0/3V)\mu \quad (2.3)$$

is the coupling constant, and κ^{-1} is the roundtrip transit time of the photons in the cavity times T ,

$$\kappa = cT/2L. \quad (2.4)$$

In writing Eqs. (2.2) we have extracted a rapidly varying factor $\exp(-i\omega_0 t)$ from S , E , and E_I . The field E_T transmitted by the cavity is given by

$$E_T = \sqrt{T}E, \quad (2.5)$$

while the field E_R reflected by the cavity is complementary to the transmitted field

$$E_R^2 = (E_I - E_T)^2. \quad (2.6)$$

The coherent terms in Eqs. (2.2) describe the interaction between the field and the atoms in the dipole and rotating wave approximation, while the incoherent terms describe the atomic decay and the escape of photons from the cavity (propagation). In particular, the damping term in Eq. (2.2c) arises from propagation and from the boundary conditions (see Appendix A). Its structure can be intuitively understood as follows. When the cavity is empty of atomic material ($\mu=0$) the stationary solution of Eq. (2.2c) is

$$E = E_I/\sqrt{T},$$

i.e., $E_T = E_I$ by Eq. (2.5). This is the usual situation for an empty Fabry-Perot perfectly tuned to the incident field. E_I is a fixed constant which we assume for definiteness to be $E_I \geq 0$. Putting $E_I = 0$ and replacing $-\frac{1}{2}N$ by a positive inversion our Eqs. (2.2) reduce to the one-mode laser model in a ring laser cavity in the semiclassical approximation.² Furthermore, Eqs. (2.2) with $E_I = 0$ and $R = 0$ (cavity without mirrors) reduce to the mean-field model for superfluorescence again in the semiclassical approximation.⁷ Hence Eqs. (2.2) generalize these physical situations to include the effect of the injected field.

The reaction field is given by

$$E_{\text{react}} = E - E_I/\sqrt{T} = (E_T - E_I)/\sqrt{T} = E_R/\sqrt{T}, \quad (2.7)$$

where Eqs. (2.5) and (A16) have been used. Furthermore from Eq. (2.2c) one has that in the stationary situation ($\dot{E} = 0$)

$$E_{\text{react}} = -(g/\kappa)S. \quad (2.8)$$

These equations link the reaction field, the absorption [Eq. (2.8)], and the reflection [Eq. (2.7)].

Equations (2.2) can be rewritten as follows:

$$\dot{S} = (\mu/\hbar)[E_{\text{react}} + (E_I/\sqrt{T})]\Delta - \gamma_{\perp}S, \quad (2.9a)$$

$$\dot{\Delta} = -(\mu/\hbar)[E_{\text{react}} + (E_I/\sqrt{T})]S - \gamma_{\parallel}(\Delta - \frac{1}{2}N), \quad (2.9b)$$

$$\dot{E}_{\text{react}} = -gS - \kappa E_{\text{react}}. \quad (2.9c)$$

Neglecting the reaction field, i.e., setting $E_{\text{react}} = 0$, the atomic equations (2.9a) and (2.9b) become a closed system of linear equations for S and Δ which coincide with the equations for resonance fluorescence (in the case of exact resonance and for $T=1$) studied in Ref. 9(a). In these works⁹ resonance fluorescence is described as the interaction of the external radiation field with a *single* atom, assuming that the atoms evolve independently of one another, so that S and Δ are simply proportional to N . On the contrary, in the present paper we take into account the cooperative effects arising from radiation reaction via the *nonlinear* terms in Eqs. (2.9). We stress, finally, that Eqs. (2.2) can be easily deduced from a fully quantum-mechanical model using the semiclassical approximation. Such a model is a simple generalization of the one-mode laser model with running wave.² The derivation is shown in Appendix B. The availability of a quantum-mechanical model is very important since a rigorous discussion of the spectrum of the fluorescent light requires a fully quantum-mechanical treatment.

III. STATIONARY SOLUTIONS AND BISTABILITY

Let us now look for the steady-state solutions of Eqs. (2.3) (i.e., $\dot{S} = \dot{\Delta} = \dot{E} = 0$). For this purpose it is convenient to introduce the Rabi frequencies¹⁰ Ω_T and Ω_I in the total internal field and in the incident field, respectively:

$$\Omega_T = \mu E/\hbar = (1/\sqrt{T})(\mu E_T/\hbar), \quad (3.1)$$

$$\Omega_I = (1/\sqrt{T})(\mu E_I/\hbar),$$

where we have used Eq. (2.5). Similarly, let us define the saturation parameters x and y in the total field and in the incident field, respectively:

$$x = \Omega_T/(\gamma_{\perp}\gamma_{\parallel})^{1/2}, \quad y = \Omega_I/(\gamma_{\perp}\gamma_{\parallel})^{1/2}. \quad (3.2)$$

Now in the stationary situation, Eqs. (2.2a) and (2.2b) give the typical expressions of S and Δ in terms of x :

$$S = \frac{1}{2}N \left(\frac{\gamma_{\parallel}}{\gamma_{\perp}} \right)^{1/2} \frac{x}{1+x^2} \equiv S_{\text{max}} \frac{2x}{1+x^2}, \quad (3.3a)$$

$$\Delta = \frac{1}{2}N \frac{1}{1+x^2}, \quad (3.3b)$$

$$N_2 = \frac{1}{2}N - \Delta = \frac{1}{2}N \frac{x^2}{1+x^2}. \quad (3.3c)$$

On the other hand, inserting (3.3a) into Eq. (2.2c) with $\dot{E} = 0$ one gets the "state equation" which for any given y (i.e., for any given E_I) fixes the stationary values of x (i.e., of E_T):

$$y = x + 2Cx/(1+x^2), \quad (3.4)$$

where

$$C = \frac{\gamma_R}{2\gamma_L}, \quad \gamma_R = \frac{\mu g N}{2\hbar\kappa} = \frac{2\pi\omega_p \mu^2 N}{3V\hbar\kappa}. \quad (3.5)$$

We note that for $R=0$, $\tau_R = \gamma_R^{-1}$ is the characteristic time of superfluorescence.⁷ In the case of pure (i.e., single pulse) superfluorescence, the time duration of the hyperbolic secant pulse is $\sim 2\tau_R$, so that γ_R is the cooperative linewidth. Hence C is the ratio between a cooperative and a noncooperative decay rate. The expression (3.5) of γ_R can be rewritten as⁷

$$\gamma_R = \gamma\rho L\lambda^2/8\pi(1-R), \quad (3.6)$$

where γ is the natural linewidth, λ_0 the wavelength and $\rho = N/V$ the atomic density. On the other hand, taking into account the relation which links γ_R , γ , and the absorption coefficient α_{abs} ,¹¹ one has

$$C = \alpha_{\text{abs}}L/2(1-R). \quad (3.7)$$

The parameter C is controlled by varying the density ρ , the length L , and the reflectivity R . In the one-atom theory (i.e., $E_{\text{react}} = 0$, so that $E_T = E_I$), by definition [cf. (3.1), (3.2)] $x = y$, which is the solution of Eq. (3.4) if one neglects the term with C . In this case, we see from Eqs. (3.3) that S , Δ , and N_2 are proportional to N . Hence the term containing C in Eq. (3.4) describes atomic cooperation, as is also apparent from the fact that C is proportional to the cooperative linewidth γ_R . Since $\gamma_R \propto N$, the solutions of Eq. (3.4) depend in general on N , so that when the term with C is important S , Δ , and N_2 are no longer extensive quantities. The physical interpretation of Eq. (3.4) is clear. In fact, taking into account Eqs. (3.1) and (3.2) we see that Eq. (3.4) can be rephrased as

$$E_I = E_T + 2CE_T/(1 + E_T^2/I_s), \quad (3.4')$$

where $I_s = \mu^2/T\hbar^2\gamma_L\gamma_{\parallel}$ is the saturation intensity. Clearly the cooperative term describes absorption from the atomic system. It is a nonlinear absorption term which gives rise to all the interesting features of the present model.¹² It has a typical saturable absorption structure which stems from the dependence of S on the saturation parameter x . In fact, in the saturation region $x \gg 1$ the cooperative term is negligible, whereas in the unsaturated region it is relevant and can dramatically

change the physical picture given by the one-atom theory. To obtain the dependence of E_T on E_I one must invert the function $y(x)$ given by Eq. (3.4). This amounts to solving a cubic algebraic equation, so that E_T can be a multivalued function of E_I . More specifically, the function $y(x)$ has a qualitatively different shape according to whether $C > 4$ or $C < 4$ (see Fig. 2). In other words, $C = 4$ is a critical value which separates two physically distinct situations. In fact, for $C < 4$, y is a monotonic function of x , so that the inverse function $x = x(y)$ is single valued. So the transmitted light increases monotonically and continuously with the incident light. Also, the other physical quantities which are continuous functions of x (as, e.g., the total fluorescence intensity I_F which is proportional to the population of the upper level N_2) vary continuously with the incident light. Hence in this case the physical picture is not qualitatively different from that given by the one-atom theory. The only relevant difference is the presence of a region in which the differential gain dE_T/dE_I exceeds unity, i.e., where $dy/dx < 1$. This phenomenon has been experimentally checked in Ref. 6.¹³

On the other hand, for $C > 4$ the function (3.4) has one maximum x_M , and one minimum x_m , given by

$$x_M = \left(\frac{2C+1}{C-1+(C^2-4C)^{1/2}} \right)^{1/2}, \quad (3.8a)$$

$$x_m = [C-1+(C^2-4C)^{1/2}]^{1/2}. \quad (3.8b)$$

Hence x is a multivalued function of y . In fact, Eq. (3.4) has one solution x_1 for $y < y_m$, three solutions $x_1 < x_2 < x_3$ for $y_m < y < y_M$ and one solution x_3 for $y > y_M$. We stress that exchanging ordinates with abscissas

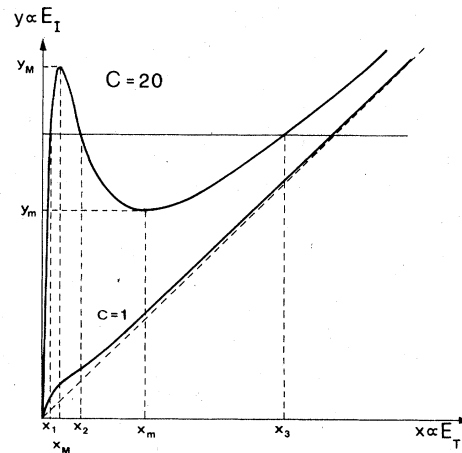


FIG. 2. Plot of the function $y = x + 2Cx/(1+x^2)$ for $C=1$ and $C=20$. For $C \gg 1$ one has $x_M \approx 1$, $y_M \approx C$, $x_m \approx \sqrt{2C}$, and $y_m \approx \sqrt{8C}$. Points x_1 and x_3 are stable, points x_2 are unstable.

in Fig. 2 for $C > 4$ one obtains a graph which closely resembles the numerical plot of E_T vs E_I given in Ref. 5. In the following, we shall consider the situation $C \gg 1$ in which the maximum and the minimum are well pronounced and separated. In this situation, one has

$$\begin{aligned} x_M &\simeq 1, \quad y_M \simeq C, \\ x_m &\simeq \sqrt{2C}, \quad y_m \simeq \sqrt{8C}. \end{aligned} \quad (3.9)$$

The stationary solution x_1 can be approximately calculated neglecting the term x in Eq. (3.4). This gives

$$x_1 = y / [C + (C^2 - y^2)^{1/2}]. \quad (3.10)$$

For $y < y_m \simeq \sqrt{8C}$, one has the linear relation $x_1 \simeq y/2C \ll 1$. In particular, for $y \simeq \sqrt{8C}$, $x_1 \simeq \sqrt{2}/C$. On the other hand, the stationary solution x_3 can be approximately calculated by neglecting 1 with respect to x^2 in the cooperative term of Eq. (3.4). One obtains

$$x_3 = \frac{1}{2}y[1 + (1 - 8C/y^2)^{1/2}]. \quad (3.11)$$

In particular, for $y > y_M \simeq C$ one has the linear relation $x_3 \simeq y \gg 1$. The linear stability analysis performed in the next section shows that points x_1 and x_3 are stable, whereas points x_2 are unstable. Since, for $y > C$, x_3 practically coincides with the one-atom solution, we shall call x_3 "one-atom stationary state." On the other hand, point x_1 arises from atomic cooperation, so that we term it "cooperative stationary state." So for $C > 4$ and $y_m < y < y_M$ the system is bistable, and it is easy to see how the hysteresis cycle of E_T vs E_I arises. In fact, one must simply erase from the plot of Fig. 2 ($C > 4$) the part with negative slope (i.e., the part corresponding to the unstable points x_2) and exchange the axes x and y in order to have a plot of transmitted light versus incident light. In such a way one obtains Fig. 1. The discontinuous changes occur when the system jumps from the cooperative to the one-atom stationary state or vice versa. The transition points $y_m \simeq \sqrt{8C}$ and $y_M \simeq C$ correspond to $\Omega_I \simeq 2(\gamma_R \gamma_L)^{1/2}$ and $\Omega_I \simeq \frac{1}{2}\gamma_R(\gamma_L \gamma_L)^{1/2}$ respectively. Note that the jump is of a factor C at both transition points (see Fig. 1).

Clearly from Eqs. (3.3) we see that one finds a hysteresis cycle in all other relevant physical quantities. In fact, using Eqs. (3.3) and (3.11) we see that when the system is in the one-atom stationary state x_3 , which corresponds to practically complete saturation (i.e., $x_3 \gg 1$) one has

$$S_3 \simeq \frac{1}{2}N \left(\frac{\gamma_{\parallel}}{\gamma_{\perp}} \right)^{1/2} \frac{1}{x_3} = \left(\frac{\gamma_{\parallel}}{\gamma_{\perp}} \right)^{1/2} \frac{N}{y} \frac{1}{1 + (1 - 8C/y^2)^{1/2}}, \quad (3.12a)$$

$$N_2^{(s)} \simeq \frac{1}{2}N. \quad (3.12b)$$

In particular, for $y \simeq y_m \simeq \sqrt{8C}$ one has

$$S_3 \simeq (\gamma_{\parallel}/\gamma_{\perp})^{1/2} [N/(8C)^{1/2}] \simeq \Omega_I/2I_1, \quad (3.13a)$$

where we have introduced the notation

$$I_1 = \mu g / \hbar \kappa = 4\pi\omega_0\mu^2 / 3V\hbar\kappa, \quad (3.14)$$

so that $\gamma_R = I_1 \frac{1}{2}N$ and

$$2C = I_1 N / 2\gamma_{\perp}. \quad (3.14')$$

To derive the last term of Eq. (3.13a) we have used Eqs. (3.2) and (3.14'). For $y = y_M \simeq C \gg 1$ Eq. (3.12a) gives [cf. Eq. (3.3a)]

$$S_3 \simeq S_{\max}(2/C). \quad (3.13b)$$

Note that in this regime S and N_2 are proportional to N , which is the normal situation. On the other hand, from Eqs. (3.3) and (3.10) we see that when the system is in the cooperative stationary state x_1 one has

$$S_1 = (Ny/4C)(\gamma_{\parallel}/\gamma_{\perp})^{1/2} = \Omega_I/I_1, \quad (3.15a)$$

$$N_2^{(1)} = (N/4C^2)\{y^2/[1 + (1 - y^2/C^2)^{1/2}]\}, \quad (3.15b)$$

where to deduce the last term of (3.15a) we have used (3.2) and (3.14'). Note the linear dependence of S_1 on y . In particular, for $y = y_m \simeq \sqrt{8C}$ one has

$$N_2^{(1)} \simeq N/C, \quad (3.16a)$$

where for $y = y_M \simeq C$ one has

$$N_2^{(1)} \simeq \frac{1}{4}N, \quad S_1 \simeq S_{\max}. \quad (3.16b)$$

Note that since $C \propto N$ in this regime S turns out to be independent of N and N_2 is inversely proportional to N . This means that the total fluorescence intensity I_F , which is proportional to N_2 , is inversely proportional to the number of atoms. This is a striking cooperative effect. Furthermore from Eqs. (3.1), (3.2), and (3.10) we also see that in the cooperative stationary state the transmitted field amplitude is inversely proportional to the number of atoms (whereas in the one-atom stationary state one practically has $E_T = E_I$ independent of N). The physical interpretation of this cooperative behavior of the quantities E_T , S , and I_F in the state x_1 is as follows. In the bistable situation, the system has two possibilities. The first possibility is that the incident field E_I interacts with the single atoms separately (one-atom stationary state). In other words, the interaction of the incident field with each atom is unaffected by the presence of the other atoms. In this case, since the saturation parameter y of the incident field is large, the atoms get saturated so that the absorption is negligible and the medium is practically transparent. The second possibility is that the incident field interacts with the atomic system as a whole (cooperative stationary state). The

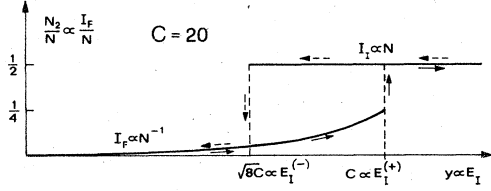


FIG. 3. Hysteresis cycle of the fluorescence intensity per atom. Full (dotted) line arrows indicate the variation obtained increasing (decreasing) the input field E_I . The upper part of the plot corresponds to the one-atom stationary state x_3 .

atoms cooperatively create a reaction field which counteracts the incident field. In this case, E_I is strongly absorbed and hence reflected [cf. Eqs. (2.7) and (2.8)], so that the transmission is very low. In such a situation an increase of the number of atoms enhances the absorption. Hence, in the limit of large N with fixed E_I the incident light gets more and more completely absorbed; this explains why in the cooperative stationary state for $C \gg 1$, S is practically independent of N . Equations (2.7), (2.8), and (3.15a) show that this situation corresponds to practically complete reflection $E_R = -E_I$. Simultaneously the transmitted and fluorescent light tend to vanish in the limit of large N .

The hysteresis cycles of I_F and S vs E_I are shown in Figs. 3 and 4, respectively. Note that the jumps are at least of a factor of 2 both for S and for I_F .

IV. LINEAR STABILITY ANALYSIS AND CRITICAL SLOWING DOWN

Not to overburden the notations, we shall indicate by S , Δ , and E the generic stationary solution of Eqs. (2.2) and by δS , $\delta \Delta$, and δE the corresponding deviations from the stationary values. Retaining only the terms which are linear in δS , $\delta \Delta$, and δE one obtains, from Eqs. (2.2), the

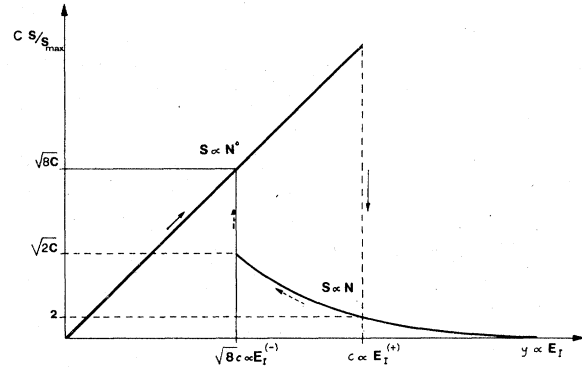


FIG. 4. Hysteresis cycle of the polarization. Arrow convention as in Figs. 1 and 3. The part of the plot beginning from the origin corresponds to the cooperative stationary state x_1 , while the other branch corresponds to the one-atom stationary state. S_{\max} is defined as $\frac{1}{4}N(\gamma_{\parallel}/\gamma_{\perp})^{1/2}$.

following set of linearized equations:

$$\delta \dot{S} = -\gamma_{\perp} \delta S + (\mu/\hbar)E \delta \Delta + (\mu/\hbar)\Delta \delta E, \quad (4.1a)$$

$$\delta \dot{\Delta} = -(\mu/\hbar)E \delta S - \gamma_{\parallel} \delta \Delta - (\mu/\hbar)S \delta E, \quad (4.1b)$$

$$\delta \dot{E} = -g \delta S - \kappa \delta E. \quad (4.1c)$$

Let us look for solutions of the type

$$\begin{bmatrix} \delta S \\ \delta \Delta \\ \delta E \end{bmatrix} = e^{\lambda t} \begin{bmatrix} \delta S_0 \\ \delta \Delta_0 \\ \delta E_0 \end{bmatrix}. \quad (4.2)$$

The system (4.1) admits nontrivial solutions only if λ is an eigenvalue of the matrix

$$M = \begin{bmatrix} -\gamma_{\perp} & (\mu/\hbar)E & (\mu/\hbar)\Delta \\ -(\mu/\hbar)E & -\gamma_{\parallel} & -(\mu/\hbar)S \\ -g & 0 & -\kappa \end{bmatrix}. \quad (4.3)$$

The characteristic equation $\det(M - \lambda I) = 0$ gives

$$\lambda^3 + (\gamma_{\perp} + \gamma_{\parallel} + \kappa)\lambda^2 + [\gamma_{\perp}\gamma_{\parallel} + \kappa\gamma_{\perp} + \kappa\gamma_{\parallel} + (\mu/\hbar)g\Delta + (\mu^2/\hbar^2)E^2]\lambda + \kappa\gamma_{\perp}\gamma_{\parallel} + (\mu/\hbar)g\gamma_{\parallel}\Delta + (\mu^2/\hbar^2)\kappa E^2 - (\mu^2/\hbar^2)gES = 0. \quad (4.4)$$

Taking into account that in the stationary state

$$E = -(g/\kappa)S + (E_I/\sqrt{T}), \quad (4.5)$$

and using (3.1) and (3.14), we see that Eq. (4.4) becomes

$$\lambda^3 + a_2\lambda^2 + a_1\lambda + a_0 = 0, \quad (4.6)$$

$$a_2 = \gamma_{\perp} + \gamma_{\parallel} + \kappa, \quad (4.7a)$$

$$a_1 = \gamma_{\perp}\gamma_{\parallel} + \kappa\gamma_{\perp} + \kappa\gamma_{\parallel} + \kappa I_1 \Delta + (\Omega_I - I_1 S)^2, \quad (4.7b)$$

$$a_0 = \kappa[\gamma_{\perp}\gamma_{\parallel} + \gamma_{\parallel} I_1 \Delta + (\Omega_I - I_1 S)(\Omega_I - 2I_1 S)]. \quad (4.7c)$$

The stationary solution is stable if and only if all the roots of Eq. (4.6) have a negative real part. As it is shown in Appendix C, using the extended Routh-Hurwitz theorem¹⁴ one sees that the stability condition for this problem is simply

$$a_0 > 0. \quad (4.8)$$

Now inserting into (4.7c) the expressions (3.3a) and (3.3b) for S and Δ , and taking into account that

$$\gamma_{\perp}\gamma_{\parallel} + \frac{\gamma_{\parallel}I_1N}{2(1+x^2)} + \left[(\gamma_{\perp}\gamma_{\parallel})^{1/2} \left(x + \frac{2Cx}{1+x^2} \right) - \left(\frac{\gamma_{\parallel}}{\gamma_{\perp}} \right)^{1/2} \frac{I_1Nx}{2(1+x^2)} \right] \left[(\gamma_{\perp}\gamma_{\parallel})^{1/2} \left(x + \frac{2Cx}{1+x^2} \right) - \left(\frac{\gamma_{\parallel}}{\gamma_{\perp}} \right)^{1/2} \frac{I_1Nx}{1+x^2} \right] > 0. \quad (4.10)$$

Using the relation (3.14') one verifies by straightforward algebra that (4.10) reduces to

$$(1+x^2)^2 + 2C(1-x^2) > 0. \quad (4.11)$$

Equation (4.11) is precisely the condition

$$dy/dx > 0. \quad (4.12)$$

Hence a solution of the stationary equation (3.4) is stable if and only if it lies on a part of the plot $y(x)$ with positive slope. This proves what was anticipated, i.e., that points x_1 and x_3 are stable, whereas points x_2 are unstable. The stability condition (4.8) can be immediately used to establish an important result, i.e., the existence of a critical slowing down in correspondence with the transition points y_M , y_m (i.e., $E_I^{(+)}$, $E_I^{(-)}$). This critical slowing down is similar to that which occurs in tunnel diodes.¹⁵ In fact, let $a_0^{(1)}$ be the coefficient a_0 appearing in the characteristic equation (4.6) for the stationary solution x_1 . As $y \rightarrow y_M$ one has that $x_1 \rightarrow x_M$ and that $y'(x_1) \rightarrow 0$. From what we just demonstrated

$$dy/dx \gtrless 0 \Leftrightarrow a_0 \gtrless 0,$$

so that

$$a_0^{(1)} - 0 \text{ for } y - y_M. \quad (4.13)$$

Hence one of the roots (and only one, because a_1 is always positive) of the characteristic equation (4.6) corresponding to the stationary solution x_1 tends to zero as $y \rightarrow y_M$. This means that the cooperative stationary solution x_1 exhibits a critical slowing down as E_I approaches the transition point $E_I^{(+)}$ from below. In fact, the roots of the characteristic equation (4.6) give the rate with which the system returns to the stationary state once it has been slightly removed from it. Hence as E_I approaches $E_I^{(+)}$ from below the system returns to the stationary state x_1 more and more slowly. This phenomenon concerns all the physical quantities, i.e., S , Δ , N_2 , E , and in particular the transmitted light. The proof of the existence of a critical slowing down as E_I approaches $E_I^{(-)}$ from above is completely analogous.

V. TRANSIENT BEHAVIOR

Let us consider a stable stationary state of our system. If at a given time the state of the system

by (3.2) and (3.4),

$$\Omega_I = (\gamma_{\perp}\gamma_{\parallel})^{1/2} \left\{ x + [2Cx/(1+x^2)] \right\}, \quad (4.9)$$

we see that condition (4.8) becomes

differs slightly from this stationary state, the approach to the steady situation is ruled by the three exponentials $\exp(\lambda_i t)$ ($i = a, b, c$), where λ_i are the roots of the characteristic equation (4.6). The initial deviation from the stationary state can arise either from an *external perturbation* or from a *spontaneous fluctuation* of the system. In this section we discuss the first possibility, i.e., the *transient* behavior of the system. On the other hand, in Sec. VI we shall illustrate the possible implications of the linear analysis with respect to the spectrum of the fluorescent light, which arises from the fluctuation in the *stationary* situation. The transient behavior can be experimentally studied in the following way. Let us assume that the system is initially in a stable steady state corresponding to some value E_I of the external field. If E_I is suddenly changed into $E_I + \delta E_I$ ($|\delta E_I| \ll E_I$) the system approaches the new slightly different steady state corresponding to $E_I + \delta E_I$. This approach is described by a solution of Eqs. (4.1) and can be experimentally observed by looking at the transient behavior of the transmitted light.

Let us now analyze the roots of the characteristic equation (4.6). We have approximately solved Eq. (4.6) for both stable steady states x_1 and x_3 in the neighborhood of the transition points y_m and y_M . We have done this for $C \gg 1$, neglecting higher-order corrections in C^{-1} . Since the zeroth-order term a_0 in Eq. (4.6) vanishes for $\{y = y_M, x = x_M\}$ and $\{y = y_m, x = x_m\}$ due to the critical slowing down, the value of x_1 for $y = y_M - \epsilon$ and the value of x_3 for $y = y_m + \epsilon$ must be evaluated with some accuracy. This evaluation is explicitly given in Appendix D. The analysis of Eq. (4.6) in the four cases

$$\begin{aligned} \{y \simeq y_m, x = x_1\}, \quad \{y = y_M - \epsilon, x = x_1\}, \\ \{y \gtrsim y_M, x = x_3\}, \quad \{y = y_m + \epsilon, x = x_3\}, \end{aligned}$$

is shown, instead, in Appendix E. Here we simply review the results and comment on them. Let us first consider the case

$$\kappa \gg \gamma_{\perp}, \gamma_{\parallel}. \quad (5.1)$$

This situation characterizes superfluorescence as opposed to the usual laser systems.

(i) $y \simeq y_m \simeq \sqrt{8C}$, $x = x_1$. Within higher-order corrections in C^{-1} , one finds the three roots

$$\lambda_a = -\gamma_{\parallel}, \quad \lambda_b = -\gamma_R, \quad \lambda_c = -\kappa \quad (5.2)$$

for $\kappa \gg \gamma_R$, and

$$\lambda_a = -\gamma_{\parallel}, \quad \lambda_b = -\frac{1}{2}\kappa \pm i(\kappa\gamma_R)^{1/2} \quad (5.2')$$

for $\kappa \gg \gamma_R$.

(ii) $y = y_M - \epsilon \approx C - \epsilon$, $x = x_1$. In this case one finds

$$\begin{aligned} \lambda_a &= -2\gamma_{\parallel} \frac{[1 - (y^2/C^2)]^{1/2}}{1 + [1 - (y^2/C^2)]^{1/2}}, \\ \lambda_b &= -\frac{1}{2}\gamma_R [1 + [1 - (y^2/C^2)]^{1/2}], \quad \lambda_c = -\kappa \end{aligned} \quad (5.3)$$

for $\kappa \gg \gamma_R$, and

$$\begin{aligned} \lambda_a &= -2\gamma_{\parallel} \frac{[1 - (y^2/C^2)]^{1/2}}{1 + [1 - (y^2/C^2)]^{1/2}}, \\ \lambda_{b,c} &= -\frac{1}{2}\kappa \pm i \left(\frac{1}{2}\kappa\gamma_R [1 + [1 - (y^2/C^2)]^{1/2}] \right)^{1/2} \end{aligned} \quad (5.3')$$

for $\kappa \ll \gamma_R$. Note that (5.3) and (5.3') reduce (5.2) and (5.2') for $y/C \ll 1$.

(iii) $y \approx y_M \approx C$, $x = x_3$. One gets the roots

$$\begin{aligned} \lambda_{a,b} &= -\frac{1}{2}(\gamma_{\perp} + \gamma_{\parallel}) \pm i\Omega_I, \\ \lambda_c &= -\kappa. \end{aligned} \quad (5.4)$$

The result (5.4) is independent of the assumption (5.1).

(iv) $y = y_m + \epsilon \approx \sqrt{8C} + \epsilon$, $x = x_3$. One obtains

$$\begin{aligned} \lambda_a &= -\frac{1}{2}\Omega_I^2 \frac{[(y^2/8C) - 1]^{1/2}}{2\gamma_{\perp} + \gamma_{\parallel} - 2\gamma_{\perp}[(y^2/8C) - 1]^{1/2}}, \\ \lambda_b &= -[2\gamma_{\perp} + \gamma_{\parallel} - 2\gamma_{\perp}[(y^2/8C) - 1]^{1/2}], \\ \lambda_c &= -\kappa, \end{aligned} \quad (5.5)$$

for $\kappa\gamma_{\perp}, \kappa\gamma_{\parallel} \gg \Omega_I^2$ and one obtains

$$\begin{aligned} \lambda_a &= -2\kappa \frac{[(y^2/8C) - 1]^{1/2}}{1 + 2[(y^2/8C) - 1]^{1/2}}, \\ \lambda_{b,c} &= -\frac{1}{2}\kappa \left(1 - \frac{2[(y^2/8C) - 1]^{1/2}}{1 + 2[(y^2/8C) - 1]^{1/2}} \right) \\ &\quad \pm i \frac{1}{2}\Omega_I \left[1 + 2[(y^2/8C) - 1]^{1/2} \right]^{1/2} \end{aligned} \quad (5.5')$$

for $\kappa \ll \Omega_I$. On the basis of Eqs. (5.2)–(5.5') we can now discuss the hysteresis cycle in the transient behavior. Since the damping constants λ_a , λ_b , and λ_c are well separated the approach to the stationary state is mainly characterized by the slowest decaying exponential $\exp(\bar{\lambda}t)$. In all the four cases considered one has $\bar{\lambda} = \lambda_a$. Hence, from Eqs. (5.2), (5.2'), (5.3), and (5.3'), we see that the approach to the cooperative stationary state is monotonic, because $\bar{\lambda}$ is real. Approaching the value $y_m \approx C$ from below the rate constant $\bar{\lambda}$ tends to zero (critical slowing down) as $(y_m - y)^{1/2}$. At the transition value $y = y_m$ the rate constant $\bar{\lambda}$ changes discontinuously and becomes complex [see Eq. (5.4)]. Hence the approach to the one-atom stationary state for $y \gtrsim y_m$ is oscillatory. The rate of approach is given by the mean value of the

relaxation rates $\gamma_{\perp}, \gamma_{\parallel}$ while the frequency of oscillation is the Rabi frequency Ω_I . Let us now decrease the incident field starting from values $E_I > E_I^{(*)}$ (i.e., $y > y_m$). Since $\bar{\lambda} = \lambda_a$ is real in the neighborhood of $y = y_m + \epsilon$ [cf. Eqs. (5.5) and (5.5')], the oscillatory character of the approach to the one-atom stationary state continuously disappears as y is decreased from y_m to y_m . Furthermore, approaching the value $y_m \approx \sqrt{8C}$ from above $\bar{\lambda}$ tends to zero (critical slowing down) as $(y - y_m)^{1/2}$. Finally crossing the transition value $y = y_m$, the rate constant $\bar{\lambda}$ suddenly jumps to the value $\bar{\lambda} = -\gamma_{\parallel}$, closing the cycle. The hysteresis of the real and imaginary part of the rate constant $-\bar{\lambda}$ is shown in Fig. 5.

We note that when k is dominant over all the other characteristic rates in play (i.e., not only $\gamma_{\perp}, \gamma_{\parallel}$ but also Ω_I, γ_R) the field E can be adiabatically eliminated from the model equations (2.2) [i.e., one can put $\dot{E} = 0$ in Eqs. (2.2c)], obtaining the two

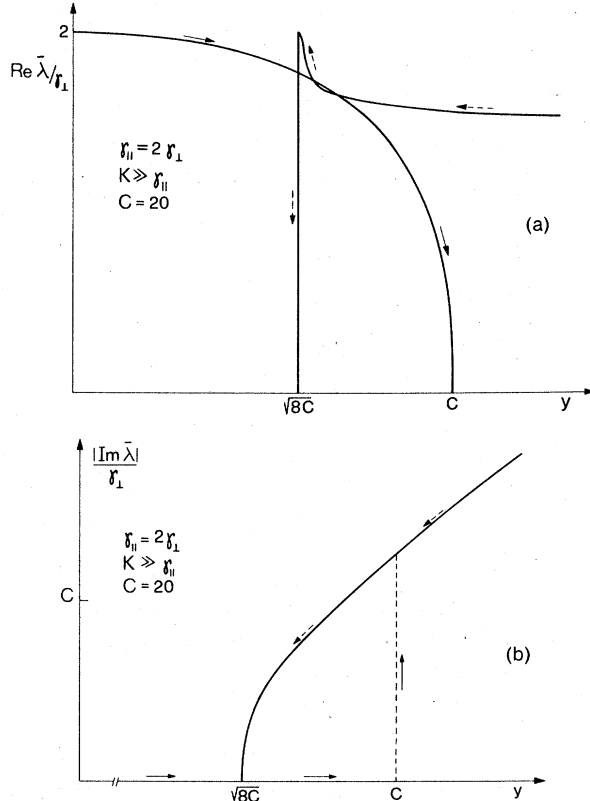


FIG. 5. Behavior of (a) the real part, and (b) the imaginary part, of the damping constant $\bar{\lambda}$, which characterizes the approach to the stationary state. Arrow convention as in Figs. 1 and 3. The part of the plot beginning from the left corresponds to the cooperative stationary state x_1 . For $y > C \gg 1$ one has that $|\text{Im } \bar{\lambda}| \approx \Omega_I \gg |\text{Re } \bar{\lambda}| \approx \gamma_{\perp}$. Decreasing the incident field, $\text{Im } \bar{\lambda}$ vanishes when y is only very slightly larger than y_m .

closed equations for S and Δ :

$$\begin{aligned}\dot{S} &= -(2\gamma_R/N)S\Delta + \Omega_I\Delta - \gamma_\perp S, \\ \dot{\Delta} &= (2\gamma_R/N)S^2 - \Omega_I S - \gamma_\parallel(\Delta - \frac{1}{2}N).\end{aligned}\quad (5.6)$$

In this situation, one can discuss the transient behavior by linearizing Eqs. (5.6). Hence one obtains a characteristic equation of second degree, which can be solved more easily. The two roots that one obtains coincide with the roots λ_a and λ_b , given by Eqs. (5.2)–(5.5), respectively, in the cases (i)–(iv).

Let us now consider the situation

$$\kappa \ll \gamma_\perp, \gamma_\parallel. \quad (5.7)$$

In this case, we shall evaluate the damping constant $\bar{\lambda}$ by adiabatically eliminating the atomic quantities S and Δ from the model equations (2.2). Hence, using Eq. (3.2) we obtain the closed equation for $x \propto E$,

$$\dot{x} = \kappa \{ y - x - [2Cx/(1+x^2)] \}, \quad (5.8)$$

which gives the linearized equation

$$\delta\dot{x} = -\kappa \{ 1 + 2C[(1-x^2)/(1+x^2)^2] \} \delta x. \quad (5.9)$$

From Eq. (5.9) we get

$$\bar{\lambda} = -\kappa \{ 1 + 2C[(1-x^2)/(1+x^2)^2] \}. \quad (5.10)$$

Using Eq. (5.10), we obtain in the four considered cases:

$$(i) \ y \approx y_m \approx (8C)^{1/2}, \quad x = x_1:$$

$$\bar{\lambda} = -2\kappa C, \quad (5.11)$$

$$(ii) \ y = y_M - \epsilon \approx C - \epsilon, \quad x = x_1:$$

$$\bar{\lambda} = -\kappa C [1 - (y^2/C^2)]^{1/2}, \quad (5.12)$$

$$(iii) \ y \geq y_M \approx C, \quad x = x_3:$$

$$\bar{\lambda} = -\kappa \quad (5.13)$$

$$(iv) \ y = y_m + \epsilon \approx (8C)^{1/2} + \epsilon, \quad x = x_3:$$

$$\bar{\lambda} = -2\kappa [(y^2/8C) - 1]^{1/2}. \quad (5.14)$$

Hence, in the case $\kappa \ll \gamma_\perp, \gamma_\parallel$ one also obtains a hysteresis cycle for the transient behavior. The main difference from the case $\kappa \gg \gamma_\perp, \gamma_\parallel$ is that now the approach to the stationary state is always monotonic.

VI. SPECTRUM OF THE FLUORESCENT LIGHT

The description of the spectrum of the fluorescent light requires the analysis of the fluctuations (time correlation function) of the fluorescence field around the stable stationary states. As shown in Ref. 9(a), the fluctuations of the fluorescence field are in turn simply related to the fluctuations of the polarization. Of course the study of these

fluctuations requires a fully quantum-mechanical analysis. However, on the basis of the regression hypothesis we can assume that the time dependence of the polarization fluctuations in the stationary state is well reproduced by the transient approach of the polarization to the stationary state. Since we have analyzed this approach by means of the characteristic equation (4.6), we can get some information concerning the spectrum.

We recall that the presence of oscillations in the time correlation function is a necessary condition for the existence of a DSS (i.e., three-peaked spectrum) which in fact appears when the shift becomes larger than the linewidth. Hence in this spirit we shall consider as a necessary condition for the appearance of a DSS the presence of oscillations in the approach to the stationary state. More specifically, we shall tentatively estimate the linewidth of the incoherent part of the fluorescent light as $2|\text{Re}\bar{\lambda}|$ and the shifts as $|\text{Im}\bar{\lambda}|$. In the following we shall consider the case (5.1), which is more interesting. On the basis of Eqs. (5.2)–(5.4) we can now discuss the discontinuous change in the spectrum which occurs when increasing the incident field up to the transition value $y = y_M$ (i.e., $E_I = E_I^{(*)}$). Let us consider for simplicity the case $\gamma_\perp \approx \gamma_\parallel \approx \gamma$. From Eqs. (5.2)–(5.3') we see that when the system is in the cooperative stationary state x_1 the spectrum is single peaked, because the approach to x_1 is monotonic ($\bar{\lambda} = \lambda_a$, real). Furthermore one has a line narrowing ($\lambda \rightarrow 0$) as y approaches y_M from below. When crossing the transition value $y = y_M$ one has an abrupt appearance of a large DSS, which coincides with that predicted by the one-atom theory in the high-intensity limit. In fact the shift is given by the Rabi frequency Ω_I and for $\gamma_\parallel = 2\gamma_\perp$ one sees that $2|\text{Re}\lambda_{a,b}|$ coincides with the width of the sidebands as predicted in Ref. 9. These sidebands are well separated, because from Eq. (3.2) $\Omega_I = (\gamma_\perp \gamma_\parallel)^{1/2} y \approx \gamma y \approx \gamma C \gg \gamma$. Therefore the condition for the appearance of the DSS is $y > y_M \approx C$, which for $\gamma_\perp \approx \gamma_\parallel \approx \gamma$ means (neglecting factors of 2) $\Omega_I > \gamma_R$. The threshold $\Omega_I = \gamma_R$ can be well understood by referring to the Rabi frequency Ω_T of the total internal field instead of referring to the Rabi frequency Ω_I of the incident field. In fact $y > C$ corresponds to $x > 1$, which for $\gamma_\perp \approx \gamma_\parallel \approx \gamma$ means $\Omega_T > \gamma$. Now the atoms are acted upon by the total internal field, which for $y < C$ is not intense enough to give rise to a DSS. Only crossing the transition value $E_I^{(*)}$ the intensity of the internal field abruptly increases giving rise to a large DSS.

Figure 6 compares the picture one has below the critical density of atoms ($\gamma_R < \gamma$) with that which one obtains when atomic cooperation is dominant ($\gamma_R \gg \gamma$). In the latter case one has a kind of

first-order phase transition in the spectrum at the transition value $E_I^{(+)}$ (i.e., $\Omega_I = \gamma_R$).

Let us now discuss the discontinuous change in the spectrum which occurs when decreasing the incident field to the transition value $y = y_m$ (i.e., $E_I = E_I^{(-)}$). Again we refer for simplicity to the case $\gamma_{\perp} \approx \gamma_{\parallel} \approx \gamma$. We know that for $y \gtrsim y_m$ when the system is in the one-atom stationary state the spectrum is three-peaked. However, approaching the transition value $E_I^{(-)}$ from above the spectrum becomes a single narrow line, because as shown by Eqs. (5.5) and (5.5'), $\bar{\lambda} = \lambda_a$ becomes real and $\bar{\lambda} \rightarrow 0$. Therefore because of the critical slowing down one has a continuous disappearance of the DSS as $E_I \rightarrow E_I^{(-)} + \epsilon$. Let us remark that for $y \approx y_m$, $C \gg 1$ one has not only $\Omega_I \approx (\gamma_R \gamma)^{1/2} \gg \gamma$ but also $\Omega_T \approx \Omega_I \gg \gamma$ (systematically neglecting factors of 2). Hence for high density ($\gamma_R \gg \gamma$) the DSS disappears when the field is decreased much earlier than expected on the basis of the one-atom theory. This is another cooperative effect. Finally crossing the value $E_I^{(-)}$ from above one finds an abrupt change from the narrow line (5.5) and (5.5') to a line of width $2\gamma_{\parallel}$ [cf. Eqs. (5.2) and (5.2')] which is, however, still one-peaked.

Thus Eqs. (5.2)–(5.5') describe the spectral hysteresis cycle. We stress that the conclusions concerning the line narrowing for $y \rightarrow y_m - \epsilon$ and $y \rightarrow y_m + \epsilon$ are independent of the assumptions $\kappa \gg \gamma_{\perp}, \gamma_{\parallel}$, $C \gg 1$, and $\gamma_{\perp} \approx \gamma_{\parallel} \approx \gamma$. In fact, they follow simply from the existence of a critical slowing down, which has been rigorously established in Sec. IV

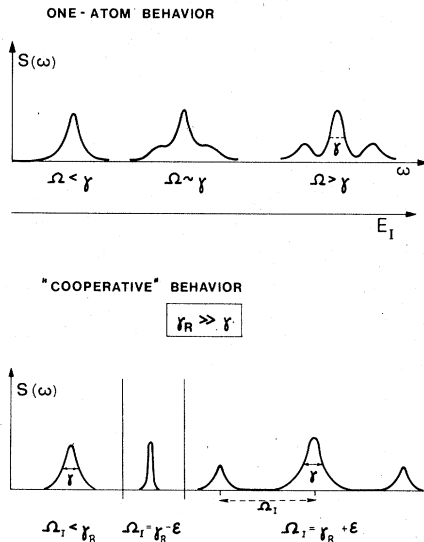


FIG. 6. Behavior of the spectrum of the fluorescent light for increasing incident field E_I when $\kappa \gg \gamma_{\perp}, \gamma_{\parallel}$, and $\gamma_{\perp} \approx \gamma_{\parallel} \approx \gamma$. For $\gamma_R < \gamma$ the DSS appears continuously when $\Omega_I \approx \gamma$, for $\gamma_R \gg \gamma$ it appears discontinuously when $\Omega_I \approx \gamma_R$.

under the only condition $C > 4$. Clearly all the statements of this section must be substantiated by a complete quantum-mechanical analysis, which should also give the analytical shape of the spectrum of the fluorescent light.¹⁶

Note added in proof. (a) After submission of this paper, we have analyzed the problem of optical bistability in a ring cavity, which does not present standing-wave effects. We have solved the Maxwell-Bloch equations at steady state, with proper boundary conditions. As a result we get an exact analytical expression for E_T as a function of E_I , which takes fully into account propagation effects. The mean-field approximation is recovered in the limit $\alpha_{\text{abs}} L \rightarrow 0$, $T \rightarrow 0$ with $\alpha_{\text{abs}} L/T = 2C$ fixed and arbitrary. In practice, for $C = 10$ the mean-field treatment turns out to be valid up to $\alpha_{\text{abs}} L \approx 1$. Hence, the predictions made in the present paper are certainly correct for a ring-laser geometry and $\alpha_{\text{abs}} L$ not too large. (b) In Sec. VI we have made some predictions concerning the spectrum of the fluorescent light. Of course the same predictions hold for the spectrum of the transmitted light, which is given by the Fourier transform of the time correlation function $\langle A^\dagger(t)A \rangle$ (see Appendix B). We have recently calculated this correlation function using the quantum-mechanical model shown in Appendix B. The result is that the spectrum of the transmitted light is composed of a coherent part proportional to the transmitted intensity and an incoherent part whose behavior fits all the predictions made in Sec. VI. These results will be discussed elsewhere.

APPENDIX A

Let $\mathcal{E}(z, t)$ be the positive frequency part of a field with central frequency ω_0 propagating in the active medium along the longitudinal axis z . The optical cavity contains N two-level atoms with transition frequency ω_0 . Let $P(z, t)$ be the macroscopic polarization field and let $D(z, t)$ be $\frac{1}{2}$ the population difference between the lower and the upper level. Let us introduce the slowly varying envelope approximation as it follows

$$\begin{aligned} \mathcal{E}(z, t) = & E_F(z, t) \exp[-i(\omega_0 t + \kappa_0 z)] \\ & + E_B(z, t) \exp[-i(\omega_0 t - \kappa_0 z)], \end{aligned} \quad (A1)$$

$$\kappa_0 = \omega_0/c,$$

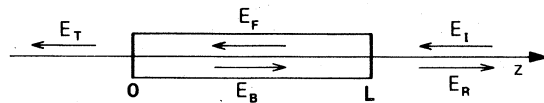


FIG. 7. E_I is the incident field. The interaction with the atoms gives rise to two fields E_F and E_B propagating in opposite directions along the z axis. E_T is the transmitted field and E_R is the reflected field.

where E_F and E_B are slowly varying fields which propagate in apposite directions as shown in Fig. 7. Correspondingly we put

$$P(z, t) = P_F(z, t) \exp[-i(\omega_0 t + \kappa_0 z)] + P_B(z, t) \exp[-i(\omega_0 t - \kappa_0 z)] + \text{c.c.}, \quad (\text{A2})$$

and

$$D(z, t) = D_0(z, t) + [D_1(z, t) \exp(-2i\kappa_0 z) + \text{c.c.}] \quad (\text{A3})$$

where P_F , P_B , D_0 , and D_1 vary slowly.

Then, if one neglects the terms proportional to $\exp(\pm 3ik_0 z)$, the slowly varying fields obey the following field-matter equations¹⁷:

$$\frac{\partial E_F}{\partial t} - c \frac{\partial E_F}{\partial z} = -g' P_F, \quad (\text{A4a})$$

$$\frac{\partial E_B}{\partial t} + c \frac{\partial E_B}{\partial z} = -g' P_B, \quad (\text{A4b})$$

$$\frac{\partial P_F}{\partial t} = \frac{\mu'}{\hbar} (E_F D_0 + E_B D_1) - \gamma_{\perp} P_F, \quad (\text{A5a})$$

$$\frac{\partial P_B}{\partial t} = \frac{\mu'}{\hbar} (E_B D_0 + E_F D_1) - \gamma_{\perp} P_B, \quad (\text{A5b})$$

$$\frac{\partial D_0}{\partial t} = -\frac{\mu'}{\hbar} (E_F P_F + E_B P_B) - \gamma_{\parallel} (D_0 - \frac{1}{2} N), \quad (\text{A5c})$$

$$\frac{\partial D_1}{\partial t} = -\frac{1}{2} \frac{\mu'}{\hbar} (E_B P_F + E_F P_B) - \gamma_{\parallel} D_1, \quad (\text{A5d})$$

where

$$g' = (4\pi\omega_0/V)\mu', \quad (\text{A5'})$$

μ' is the modulus of the atomic dipole moment and all the fields have been assumed real. The parameters γ_{\perp} and γ_{\parallel} have been defined in Sec. II. Clearly the field D_1 couples coherently the forward and backward propagating waves. The boundary conditions for Eqs. (A4a) and (A4b) corresponding to the physical situation described in Sec. II, are⁵

$$E_T(t) = \sqrt{T} E_F(0, t), \quad E_B(0, t) = \sqrt{R} E_F(0, t), \quad (\text{A6})$$

$$E_F(L, t) - \sqrt{R} E_B(L, t) = \sqrt{T} E_I, \quad (\text{A7a})$$

$$E_B(L, t) - \sqrt{R} E_F(L, t) = \sqrt{T} E_R(t), \quad (\text{A7b})$$

where E_R is the reflected field amplitude (see Fig. 7). Initially one has

$$P_F(z, 0) = P_B(z, 0) = 0,$$

$$D_0(z, 0) = \frac{1}{2} N, \quad D_1(z, 0) = 0. \quad (\text{A8})$$

For any field $F(z, t)$ we consider the spatial average $\bar{F}(t)$,

$$\bar{F}(t) = \frac{1}{L} \int_0^L dz F(z, t). \quad (\text{A9})$$

Let us now introduce the *mean field approximation*

$$\overline{FG} = \bar{F}\bar{G}, \quad (\text{A10})$$

which holds when the fields are nearly uniform. This is certainly the case when $T \ll 1$.⁶ Then integrating Eqs. (A4) and (A5) over the space and taking the boundary conditions (A6) and (A7) into account we obtain the following set of equations:

$$\dot{\bar{E}}_F - (c/L)[(R/T)^{1/2} E_R + (1/\sqrt{T})(E_I - E_T)] = -g' \bar{P}_F, \quad (\text{A11a})$$

$$\dot{\bar{E}}_B + (c/L)[(1/\sqrt{T}) E_R + (R/T)^{1/2} (E_I - E_T)] = -g' \bar{P}_B, \quad (\text{A11b})$$

$$\dot{\bar{P}}_F = (\mu'/\hbar)(\bar{E}_F \bar{D}_0 + \bar{E}_B \bar{D}_1) - \gamma_{\perp} \bar{P}_F, \quad (\text{A12a})$$

$$\dot{\bar{P}}_B = (\mu'/\hbar)(\bar{E}_B \bar{D}_0 + \bar{E}_F \bar{D}_1) - \gamma_{\perp} \bar{P}_B, \quad (\text{A12b})$$

$$\dot{\bar{D}}_0 = -(\mu'/\hbar)(\bar{E}_F \bar{P}_F + \bar{E}_B \bar{P}_B) - \gamma_{\parallel} (\bar{D}_0 - \frac{1}{2} N), \quad (\text{A12c})$$

$$\dot{\bar{D}}_1 = -(\mu'/2\hbar)(\bar{E}_B \bar{P}_F + \bar{E}_F \bar{P}_B) - \gamma_{\parallel} \bar{D}_1. \quad (\text{A12d})$$

Equations (A11) can be rephrased as follows:

$$\frac{d(\bar{E}_F + \sqrt{R} \bar{E}_B)}{dt} + \frac{c}{L} \sqrt{T} (E_T - E_I) = -g' (\bar{P}_F + \sqrt{R} \bar{P}_B), \quad (\text{A13a})$$

$$\frac{d(\sqrt{R} \bar{E}_F + \bar{E}_B)}{dt} + \frac{c}{L} \sqrt{T} E_R = -g' (\sqrt{R} \bar{P}_F + \bar{P}_B). \quad (\text{A13b})$$

To close the set of Eqs. (A12), (A13) we introduce the following two *Ansätze*:

$$(i) \bar{E}_F = \bar{E}_B \equiv E, \quad \bar{P}_F = \bar{P}_B \equiv P, \quad (\text{A14})$$

$$(ii) E = E_T / \sqrt{T}. \quad (\text{A15})$$

Clearly *Ansatz* (A14) is compatible with Eqs. (A12a) and (A12b), which reduce to one equation. Furthermore, (A14) with Eqs. (A13) implies immediately that

$$E_R = E_T - E_I. \quad (\text{A16})$$

Thus the amplitude of the reflected light is simply complementary to the transmitted light.

From the first of the boundary conditions (A6) we see that (A15) amounts to assuming for E the value of $E_F(z, t)$ at the left boundary. Both assumptions (A14) and (A15) are reasonable for $T \ll 1$.⁶ With Eqs. (A14) and (A15), Eq. (A13a) becomes

$$\dot{E} = -g' P - \kappa (E - E_I / \sqrt{T}), \quad (\text{A17})$$

where

$$\kappa = cT/L(1 + \sqrt{R}) \simeq cT/2L. \quad (\text{A18})$$

On the other hand, with Eqs. (A14) and (A15) Eqs. (A12) become

$$\dot{P} = (\mu'/\hbar) E (\bar{D}_0 + \bar{D}_1) - \gamma_{\perp} P, \quad (\text{A19a})$$

$$\dot{\bar{D}}_0 = -(2\mu'/\hbar) EP - \gamma_{\parallel} (\bar{D}_0 - \frac{1}{2} N), \quad (\text{A19b})$$

$$\dot{\bar{D}}_1 = -(\mu'/\hbar)EP - \gamma_{11}\bar{D}_1. \quad (\text{A19c})$$

Equations (A19b) and (A19c) imply that

$$\frac{d}{dt}(\bar{D}_0 - 2\bar{D}_1) = -\gamma_{11}(\bar{D}_0 - 2\bar{D}_1 - \frac{1}{2}N). \quad (\text{A20})$$

Equation (A20) with the initial condition (A8) implies in turn that

$$\bar{D}_1 = \frac{1}{2}(\bar{D}_0 - \frac{1}{2}N). \quad (\text{A21})$$

Hence introducing the quantity $\Delta = \bar{D}_0 + \bar{D}_1$ we get the following two equations:

$$\dot{P} = (\mu'/\hbar)E\Delta - \gamma_{11}P, \quad (\text{A22a})$$

$$\dot{\Delta} = -(3\mu'/\hbar)EP - \gamma_{11}(\Delta - \frac{1}{2}N). \quad (\text{A22b})$$

Finally, if one introduces the quantities

$$S = \sqrt{3}P, \quad \mu = \sqrt{3}\mu', \quad g = g'/\sqrt{3}, \quad (\text{A23})$$

Eqs. (A17), (A22a) and (A22b) reduce to our model equations (2.2).

APPENDIX B

Let A be the annihilation operator for photons of the internal field. It obeys the boson commutation relation

$$[A, A^\dagger] = 1. \quad (\text{B1})$$

Let r_i^+, r_i^- be the raising and lowering operators of the i th atom and let $r_{3i} = \frac{1}{2}(r_i^+ r_i^- - r_i^- r_i^+)$. We consider the $\frac{1}{2}$ total population inversion operator

$$R_3 = \sum_{i=1}^N r_{3i}, \quad (\text{B2})$$

and the collective dipole operators R^\pm defined as

$$R^\pm = \sum_{i=1}^N r_i^\pm \exp(\pm i\vec{k}_0 \cdot \vec{x}_i), \quad (\text{B3})$$

where \vec{k}_0 is the wave vector of the injected field and \vec{x}_i is the position of the i th atom. The operators R^\pm, R_3 obey angular momentum commutation relations

$$[R^+, R^-] = 2R_3, \quad [R_3, R^\pm] = \pm R^\pm. \quad (\text{B4})$$

We call $W(t)$ the statistical operator of the coupled system (internal field) + atoms in the interaction representation. Let $W(t)$ obey the master equation

$$\frac{dW}{dt} = -iL_{AF}W + \Lambda_F W + \Lambda_A W, \quad (\text{B5})$$

where

$$L_{AF}W = \hbar^{-1}[H_{AF}, W],$$

$$H_{AF} = i\left(\frac{2\pi\omega_0\hbar}{3V}\right)^{1/2} \mu(AR^+ - A^\dagger R^-), \quad (\text{B6})$$

$$\Lambda_F W = \kappa \{ [(A - \alpha), W(A - \alpha)^\dagger] + [(A - \alpha)W, (A - \alpha)^\dagger] \}, \quad (\text{B7})$$

$$\Lambda_A W = \sum_{i=1}^N \left\{ \frac{1}{2} \gamma_{11} [(r_i^-, W r_i^+) + [r_i^- W, r_i^+]] + (\gamma_{11} - \frac{1}{2} \gamma_{11}) [(r_{3i}, W r_{3i}) + [r_{3i} W, r_{3i}]] \right\}. \quad (\text{B8})$$

α is a fixed real number. Note that the stationary solution of Λ_F (i.e., the solution of the equation $\Lambda_F X = 0$) is the coherent state $|\alpha\rangle\langle\alpha|$. The second term in (B8) is a dephasing one. Clearly for $\alpha = 0$ (B4) reduces to the usual one-mode laser model in the case of no pumping.²

Taking into account that the mean value $\langle O \rangle$ of any observable O is given by $\text{Tr}(OW)$ and using the commutation relations (B1) and (B4) one easily deduces from Eq. (B5) the equations

$$\langle \dot{R}^- \rangle = \left(\frac{8\pi\omega_0}{3\hbar V} \right)^{1/2} \mu \langle AR_3 \rangle - \gamma_{11} \langle R^- \rangle, \quad (\text{B9a})$$

$$\langle \dot{R}_3 \rangle = - \left(\frac{2\pi\omega_0}{3\hbar V} \right)^{1/2} \mu (\langle AR^+ \rangle + \langle A^\dagger R^- \rangle) - \gamma_{11} (\langle R_3 \rangle + \frac{1}{2}N), \quad (\text{B9b})$$

$$\langle \dot{A} \rangle = + \left(\frac{2\pi\omega_0}{3\hbar V} \right)^{1/2} \mu \langle R^- \rangle - \kappa (\langle A \rangle - \alpha). \quad (\text{B9c})$$

Now, introducing the semiclassical approximation, i.e., factorizing $\langle AR_3 \rangle$ into $\langle A \rangle \langle R_3 \rangle$ etc., one obtains Eqs. (2.2) by setting

$$S = -\langle R^- \rangle = -\langle R^+ \rangle, \quad (\text{B10a})$$

$$\Delta = -\langle R_3 \rangle, \quad (\text{B10b})$$

$$E = \left(\frac{8\pi\hbar\omega_0}{3V} \right)^{1/2} \langle A \rangle = \left(\frac{8\pi\hbar\omega_0}{3V} \right)^{1/2} \langle A^\dagger \rangle, \quad (\text{B10c})$$

$$\frac{E_I}{\sqrt{T}} = (8\pi\hbar\omega_0/3V)^{1/2} \alpha. \quad (\text{B10d})$$

We mention finally that the model equations used in Ref. 4 are simply obtained from Eqs. (B9) in the semiclassical approximation using Eqs. (B10a) and (B10b), and setting

$$a = \langle A \rangle - \alpha = \langle A^\dagger \rangle - \alpha,$$

$$g = (2\pi\omega_0/3\hbar V)\mu. \quad (\text{B11})$$

Note that in the present paper the symbol g indicates a different coupling constant [cf. Eq. (2.3)].

APPENDIX C

Let us first recall the extended Routh-Hurwitz theorem, which is well known in algebra and in nonlinear mechanics.¹⁴ Consider the algebraic equation of degree n ,

$$C_0\lambda^n + C_1\lambda^{n-1} + \dots + C_n = 0, \quad (C1)$$

where the coefficients are real and $C_0 > 0$. Let the determinants D_l , $l=1, 2, \dots, n$, be defined as follows:

$$D_1 = C_1,$$

$$D_2 = \begin{vmatrix} C_1 & C_0 \\ C_3 & C_2 \end{vmatrix},$$

$$D_3 = \begin{vmatrix} C_1 & C_0 & 0 \\ C_3 & C_2 & C_1 \\ C_5 & C_4 & C_3 \end{vmatrix},$$

$$D_n = \begin{vmatrix} C_1 & C_0 & 0 & \dots & 0 \\ C_3 & C_2 & C_1 & 0 & \dots & 0 \\ & & \vdots & & & \\ C_{2n-1} & C_{2n-2} & C_{2n-3} & \dots & & C_n \end{vmatrix}.$$

Let $\mathcal{V}(\alpha_1, \alpha_2, \dots, \alpha_n)$ denote the number of changes in sign in the ordered sequence $\alpha_1, \alpha_2, \dots, \alpha_n$. Then if $D_l \neq 0$ for $l=1, 2, \dots, n$, the number P of roots of Eq. (C1) having a positive real part is given by

$$P = \mathcal{V}(C_0, D_1, D_2/D_1, D_3/D_2, \dots, D_n/D_{n-1}). \quad (C2)$$

Let us apply this theorem to our equation (4.6). We have

$$\begin{aligned} C_0 &= 1, \\ D_1 &= a_2 = \gamma_{\perp} + \gamma_{\parallel} + \kappa, \\ D_2 &= a_1 a_2 - a_0 = \gamma_{\perp}^2 \gamma_{\parallel} + \gamma_{\perp} \gamma_{\parallel}^2 + \kappa(\gamma_{\perp} + \gamma_{\parallel})^2 + \kappa^2(\gamma_{\perp} + \gamma_{\parallel}) \\ &\quad + (\gamma_{\perp} + \kappa)\kappa I_1 \Delta + (\gamma_{\perp} + \gamma_{\parallel})(\Omega_I - I_1 S)^2 \\ &\quad + \kappa(\Omega_I - I_1 S)I_1 S, \end{aligned} \quad (C3)$$

$$D_3 = a_0 D_2.$$

Now taking into account that by Eqs. (3.3) $\Delta > 0$, $S \geq 0$ and that

$$\Omega_I - I_1 S > 0, \quad (C4)$$

we see immediately that $D_2/D_1 > 0$ and that

$$D_3/D_2 > 0 \iff a_0 > 0. \quad (C5)$$

Hence, one has no root with a positive real part (stability condition) if and only if $a_0 > 0$. Equation (C4) can be proved as follows. Using Eqs. (3.2) and (3.14'), we get

$$\Omega_I/I_1 = (\gamma_{\parallel}/\gamma_{\perp})^{1/2} \frac{1}{2} N(y/2C).$$

On the other hand, Eq. (3.4) gives

$$y/2C = [x/(1+x^2)] + x/2C,$$

so that by (3.3a)

$$\Omega_I/I_1 = S + (\gamma_{\parallel}/\gamma_{\perp})^{1/2} \frac{1}{2} N(x/2C) > S,$$

which proves Eq. (C4).

APPENDIX D

Let us consider the stationary state equation (3.4) in the case that $C \gg 1$ and y is slightly smaller than y_M . The roots x_1, x_2 can be obtained by approximating the function $f(x) = x + 2Cx/(1+x^2)$ by a parabola with maximum at $x = x_M, y = y_M$; that is, we approximate Eq. (3.4) by

$$y = y_M + \frac{1}{2} f''(x_M)(x - x_M)^2. \quad (D1)$$

Since, neglecting higher-order corrections in C^{-1} , one has

$$x_M = 1 + C^{-1}, \quad y_M = C + 1, \quad f''(x_M) = -C + 3, \quad (D2)$$

Eq. (D1) is explicitly given by

$$y = C + 1 - \frac{1}{2}(C - 3)(x - 1 - C^{-1})^2. \quad (D3)$$

The solution x_1 is given by

$$x_1 = 1 + C^{-1} - (1 + \frac{3}{2} C^{-1}) \left[2 \left(1 + \frac{1}{C} - \frac{y}{C} \right) \right]^{1/2}, \quad (D4)$$

which, neglecting C^{-1} in the root and taking into account that for $y \approx y_M \approx C$ one has $2 \approx 1 + y/C$, can be rewritten as

$$x_1 = 1 + C^{-1} - (1 + \frac{3}{2} C^{-1})(1 - y^2/C^2)^{1/2}. \quad (D5)$$

Using Eqs. (3.3a) and (3.3b) and systematically neglecting higher-order corrections in C^{-1} and in $(1 - y^2/C^2)^{1/2}$, one obtains the following values of S and Δ in the stationary state x_1 :

$$S_1 = (\gamma_{\parallel}/\gamma_{\perp})^{1/2} \frac{1}{4} N \left[1 + C^{-1} (1 - y^2/C^2)^{1/2} \right], \quad (D6a)$$

$$\Delta_1 = \frac{1}{4} N \left[1 - C^{-1} + (1 + \frac{1}{2} C^{-1})(1 - y^2/C^2)^{1/2} \right]. \quad (D6b)$$

The condition $y \approx y_M \approx C + 1$ [cf. Eq. (D2)] with (3.2) and (3.14') implies that

$$\begin{aligned} (\gamma_{\parallel}/\gamma_{\perp})^{1/2} \frac{1}{4} N &\approx (\Omega_I/I_1) [1 - (1/y)] \\ &\approx (\Omega_I/I_1) (1 - C^{-1}), \end{aligned}$$

so that Eq. (D6a) can be rewritten in the manner

$$S_1 = (\Omega_I/I_1) [1 - C^{-1} + C^{-1} (1 - y^2/C^2)^{1/2}]. \quad (D7)$$

We can follow the same procedure to solve the steady-state equation (3.4) in the case that $C \gg 1$ and y is slightly larger than y_M .

The roots x_2, x_3 can be obtained by approximating Eq. (3.4) as follows:

$$y = y_m + \frac{1}{2} f''(x_m)(x - x_m)^2. \quad (D8)$$

Taking into account that, within higher-order cor-

rections in C^{-1} ,

$$\begin{aligned}x_m &= (2C)^{1/2}(1 - \frac{3}{4}C^{-1}), \\y_m &= (8C)^{1/2}(1 - \frac{1}{4}C^{-1}), \\f''(x_m) &= (2C^{-1})^{1/2}(1 - \frac{3}{4}C^{-1}),\end{aligned}$$

one obtains

$$x_3 = (2C)^{1/2}[1 - \frac{3}{4}C^{-1} + (1 + \frac{3}{8}C^{-1})(y^2/8C - 1)^{1/2}], \quad (D9)$$

from which, using (3.3a) and (3.3b),

$$S_3 = (\gamma_{\parallel}/\gamma_{\perp})^{1/2}[N/(8C)^{1/2}] \times [1 + \frac{1}{4}C^{-1} - (1 + \frac{3}{8}C^{-1})(y^2/8C - 1)^{1/2}], \quad (D10a)$$

$$\Delta_3 = N/4C[1 + C^{-1} - (2 + \frac{13}{4}C^{-1})(y^2/8C - 1)^{1/2}]. \quad (D10b)$$

The condition $y \simeq y_m \simeq (8C)^{1/2}(1 - \frac{1}{4}C^{-1})$ with (3.2) and (3.14'), gives

$$\begin{aligned}(\gamma_{\parallel}/\gamma_{\perp})^{1/2}[N/(8C)^{1/2}] &\simeq (\Omega_I/2I_1)[1 + 1/y(2C)^{1/2}] \\ &\simeq (\Omega_I/2I_1)(1 + \frac{1}{4}C^{-1}),\end{aligned}$$

so that Eq. (D10a) can be rewritten as

$$S_3 = (\Omega_I/2I_1)[1 + \frac{1}{2}C^{-1} - (1 + \frac{5}{8}C^{-1})(y^2/8C - 1)^{1/2}]. \quad (D11)$$

APPENDIX E

Let us consider Eq. (4.6) for $C \gg 1$ in the four cases considered in Sec. V.

(i) Case $y \simeq y_m \simeq \sqrt{8C}$, $x = x_1$. We assume that $\kappa \gg \gamma_{\perp}, \gamma_{\parallel}$. Using Eqs. (3.15a) and (3.16a) and neglecting higher-order terms in C^{-1} we see that Eq. (4.6) is given by

$$\lambda^3 + \kappa\lambda^2 + \kappa\gamma_R\lambda + \kappa\gamma_{\parallel}\gamma_R = 0. \quad (E1)$$

In the case $\kappa \gg \gamma_R$ we solve Eq. (E1) approximately by neglecting higher-order terms in γ_R/κ and obtain Eq. (5.2). On the other hand, for $\kappa \ll \gamma_R$ we neglect higher-order corrections in κ/γ_R and get Eq. (5.2').

(ii) Case $y = y_M - \epsilon \simeq C - \epsilon$, $x = x_1$. Assume that $\kappa \gg \gamma_{\perp}, \gamma_{\parallel}$. Using Eqs. (D6b), (D7) and neglecting

higher-order corrections in C^{-1} we see that Eq. (4.6) reduces to

$$\lambda^3 + \kappa\lambda^2 + \frac{1}{2}\kappa\gamma_R[1 + (1 - y^2/C^2)^{1/2}]\lambda + \kappa\gamma_{\parallel}\gamma_R(1 - y^2/C^2)^{1/2} = 0. \quad (E2)$$

This equation can be solved in the two opposite situations $\kappa \gg \gamma_R$ and $\kappa \ll \gamma_R$ exactly as Eq. (E1), obtaining the roots (5.3) and (5.3'), respectively.

(iii) Case $y \simeq y_M \simeq C$, $x = x_3$. Taking into account that in this case $I_1S \ll \Omega_I$, $I_1\Delta \ll \gamma_{\perp}, \gamma_{\parallel}$, and that $\gamma_{\perp}, \gamma_{\parallel} \ll \Omega_I$, Eq. (4.6) becomes

$$\lambda^3 + (\gamma_{\perp} + \gamma_{\parallel} + \kappa)\lambda^2 + (\kappa\gamma_{\perp} + \kappa\gamma_{\parallel} + \Omega_I^2)\lambda + \kappa\Omega_I^2 = 0, \quad (E3)$$

where $\Omega_I^2 \simeq \gamma_{\perp}\gamma_{\parallel}C$. Note that in this case we have not assumed $\kappa \gg \gamma_{\perp}, \gamma_{\parallel}$. We solve Eq. (E3) approximately in the two opposite situations $\kappa\gamma_{\perp}, \kappa\gamma_{\parallel} \gg \Omega_I^2$ (which implies $\kappa \gg \Omega_I$ and *a fortiori* $\kappa \gg \gamma_{\perp}, \gamma_{\parallel}$) and $\Omega_I \gg \kappa, \gamma_{\perp}, \gamma_{\parallel}$. For $\kappa\gamma_{\perp}, \kappa\gamma_{\parallel} \gg \Omega_I^2$ Eq. (E3) reduces to

$$\lambda^3 + (\gamma_{\perp} + \gamma_{\parallel} + \kappa)\lambda^2 + \kappa(\gamma_{\perp} + \gamma_{\parallel})\lambda + \kappa\Omega_I^2 = 0. \quad (E3')$$

By neglecting higher-order terms in Ω_I/κ one obtains the three approximate solutions (5.4). On the other hand, for $\Omega_I \gg \kappa, \gamma_{\perp}, \gamma_{\parallel}$ Eq. (E3) reduces to

$$\lambda^3 + (\gamma_{\perp} + \gamma_{\parallel} + \kappa)\lambda^2 + \Omega_I^2\lambda + \kappa\Omega_I^2 = 0. \quad (E3'')$$

Equation (E3'') can be easily solved by neglecting higher-order terms in κ/Ω_I , γ_{\perp}/Ω_I , and $\gamma_{\parallel}/\Omega_I$. One again obtains result (5.4).

(iv) $y = y_m + \epsilon \simeq \sqrt{8C} + \epsilon$, $x = x_3$. Assume $\kappa \gg \gamma_{\perp}, \gamma_{\parallel}$. Using Eqs. (D10b) and (D11) and neglecting higher-order corrections in C^{-1} , Eq. (4.6) reduces to

$$\begin{aligned}\lambda^3 + \kappa\lambda^2 + \{\kappa(2\gamma_{\perp} + \gamma_{\parallel}) - 2\gamma_{\perp}(y^2/8C - 1)^{1/2} \\ + \frac{1}{4}\Omega_I^2[1 + 2(y^2/8C - 1)^{1/2}]\}\lambda \\ + \frac{1}{2}\kappa\Omega_I^2(y^2/8C - 1)^{1/2} = 0. \quad (E4)\end{aligned}$$

For $\kappa\gamma_{\perp}, \kappa\gamma_{\parallel} \gg \Omega_I^2$ Eq. (E4) can be approximately solved by dropping the term $\frac{1}{4}\Omega_I^2[1 + 2(y^2/8C - 1)^{1/2}]$, obtaining the roots (5.5). On the other hand, for $\kappa \ll \Omega_I$ one can drop the term $\kappa[2\gamma_{\perp} + \gamma_{\parallel} - 2\gamma_{\perp}(y^2/8C - 1)^{1/2}]$, obtaining the result (5.5').

*Also Istituto Nazionale di Ottica, Firenze, Italy.

¹See, e.g., (a) P. Glansdorff and I. Prigogine, *Thermodynamic Theory of Structure, Stability, and Fluctuations* (Wiley, New York, 1971); (b) *Synergetics*, edited by H. Haken (Teubner, Stuttgart, 1973).

²(a) H. Haken, *Handbuch der Physik* (Springer-Verlag, Berlin, 1970), Vol. XXV/2C. (b) M. Sargent, III, M. O. Scully, and W. E. Lamb, Jr., *Laser Physics* (Addison-Wesley, Reading, Mass., 1974).

³(a) V. Degiorgio and M. O. Scully, *Phys. Rev. A* **2**,

1170 (1970); (b) R. Graham and H. Haken, *Z. Phys.* **213**, 420 (1968).

⁴R. Bonifacio and L. A. Lugiato, *Opt. Commun.* **19**, 172 (1976).

⁵S. L. McCall, *Phys. Rev. A* **9**, 1515 (1974).

⁶H. M. Gibbs, S. L. McCall, and T. N. C. Venkatesan, *Phys. Rev. Lett.* **36**, 1135 (1976).

⁷R. Bonifacio and L. A. Lugiato, *Phys. Rev. A* **11**, 1507 (1975); **12**, 537 (1975).

⁸We neglect factors of 2 and assume that $\gamma_{\perp} \simeq \gamma_{\parallel} \simeq \gamma$,

where γ_{11} is the longitudinal atomic relaxation rate.

⁹(a) B. R. Mollow, Phys. Rev. 188, 1969 (1969); (b) H. S. Carmichael and D. F. Walls, J. Phys. B 9, 1199 (1976), and references quoted therein.

¹⁰I. I. Rabi, Phys. Rev. 51, 652 (1937).

¹¹R. Friedberg and S. R. Hartmann, Phys. Lett. 37A, 285 (1971).

¹²Other optical systems in which nonlinear absorption gives rise to bistability are (i) the laser with saturable absorber, see, J. F. Scott, M. Sargent, III, and C. D. Cantrell, Opt. Commun. 15, 13 (1975); (ii) the dye laser, see, S. T. Dembinski and A. Kossakowski, Z. Phys. B 24, 141 (1976); R. B. Schaefer and C. R. Willis, Phys. Rev. A 13, 1874 (1976).

¹³Actually in the experiment of Ref. 5 nonlinear dispersion is dominant over nonlinear absorption. For the sake of simplicity in the present paper we consider the purely absorptive case (as in Ref. 5).

¹⁴M. Marden, *The Geometry of the Zeroes of a Poly-*

nomial in a Complex Variable, Math. Surveys, No. III (Amer. Math. Soc., New York, 1949).

¹⁵R. Landauer and J. W. F. Woo, in Ref. 1(b).

¹⁶After the present paper was completed, we learned that a detailed analysis of the time correlation function $\langle R^+(t)R^- \rangle$ (see Appendix B) has been recently made by G. S. Agarwal, L. M. Narducci, Da Hsuan Feng, and R. Gilmore. These authors use the quantum-mechanical model shown in Appendix B within the adiabatic elimination of the internal field variable A . The time correlation function $\langle R^+(t)R^- \rangle$ is evaluated by means of a Gaussian factorization *Ansatz*, which leads to a closed system of linear time-evolution equations for the atomic correlation functions. This analysis fully confirms all our predictions concerning the behavior of the fluctuations of the system, formulated in Sec. VI.

¹⁷See, e.g., J. A. Fleck, Jr., Appl. Phys. Lett. 13, 365 (1968).